

# Interplay of dendritic avalanches and gradual flux penetration in superconducting MgB<sub>2</sub> films

D. V. Shantsev<sup>1,2</sup>, P. E. Goa<sup>1</sup>, F. L. Barkov<sup>1,3</sup>, T. H. Johansen<sup>1,\*</sup>, W. N. Kang, and S. I. Lee<sup>4</sup>

<sup>1</sup>*Department of Physics, University of Oslo, P. O. Box 1048 Blindern, 0316 Oslo, Norway*

<sup>2</sup>*A. F. Ioffe Physico-Technical Institute, Polytekhnicheskaya 26, St.Petersburg 194021, Russia*

<sup>3</sup>*Institute of Solid State Physics, Chernogolovka, Moscow Region, 142432, Russia*

<sup>4</sup>*National Creative Research Initiative Center for Superconductivity, Department of Physics, Pohang University of Science and Technology, Pohang 790-784, Republic of Korea*

(November 15, 2018)

Magneto-optical imaging was used to study a zero-field-cooled MgB<sub>2</sub> film at 9.6 K where in a slowly increasing field the flux penetrates by abrupt formation of large dendritic structures. Simultaneously, a gradual flux penetration takes place, eventually covering the dendrites, and a detailed analysis of this process is reported. We find an anomalously high gradient of the flux density across a dendrite branch, and a peak value that decreases as the applied field goes up. This unexpected behaviour is reproduced by flux creep simulations based on the non-local field-current relation in the perpendicular geometry. The simulations also provide indirect evidence that flux dendrites are formed at an elevated local temperature, consistent with a thermo-magnetic mechanism of the instability.

## I. INTRODUCTION

The dendritic flux instability found in thin films of various superconducting materials is a striking but still poorly understood phenomenon. It consists in an abrupt penetration of magnetic flux into the superconductor along narrow branching channels which form irregular dendritic patterns on the macroscopic scale. The dendritic instability has been observed by magneto-optical (MO) imaging in films of Nb<sup>1-3</sup>, YBa<sub>2</sub>Cu<sub>3</sub>O<sub>7</sub><sup>4,5</sup> (induced by a laser pulse), and recently in MgB<sub>2</sub><sup>6-9</sup> and Nb<sub>3</sub>Sn<sup>10</sup>.

The instability is believed to be of thermomagnetic origin, similarly to the much more explored phenomenon of flux jumping.<sup>11,12</sup> Local heating due to flux motion reduces the pinning, and facilitates the further motion, which may lead to an avalanche process accompanied by a substantial temperature rise. This thermal mechanism behind dendrite formation is supported by a recent experiment, which showed that the instability can be suppressed by having a normal metal in contact with the superconductor.<sup>7</sup> Dendritic patterns of flux<sup>6</sup> and temperature<sup>13</sup> have also been obtained by simulations based on the thermal feedback mechanism.

From the thermo-magnetic nature of this instability, one expects that the critical current density  $j_c$  characterizing the flux profile across the dendritic branches reflects the elevated temperature at which they were formed. Due to a decrease of  $j_c$  with temperature, these profiles should have a less steep slope than the profiles of the regular and smooth penetration from the edges. Surprisingly, we find that in films of MgB<sub>2</sub> the flux profiles across the dendritic branches are actually much steeper. In this work we investigate this paradox, and study using MO imaging the interplay between frozen flux dendrites and the gradually advancing flux front.

## II. EXPERIMENT

Films of MgB<sub>2</sub> were fabricated on Al<sub>2</sub>O<sub>3</sub> substrates using pulsed laser deposition.<sup>14</sup> A 300 nm thick film shaped as a square with dimensions 5×5 mm<sup>2</sup> was selected for the present studies. The sample has a high degree of *c*-axis alignment perpendicular to the plane, and shows a sharp superconducting transition at  $T_c = 39$  K.

The flux density distribution in the superconducting film was visualized using MO imaging based on the Faraday effect in ferrite garnet indicator films. For a recent review of the method, see Ref. 15, and a description of our setup is found elsewhere.<sup>16</sup> The sample was glued with GE varnish to the cold finger of the optical cryostat, and a piece of MO indicator covering the sample area was placed loosely on top of the MgB<sub>2</sub> film. The gray levels in the MO images were converted to magnetic field values using a calibration curve obtained above  $T_c$ .

The MgB<sub>2</sub> film was cooled down to different temperatures  $T$  in zero magnetic field, and then a slowly increasing perpendicular field,  $B_a$ , was applied. For  $T > 10$  K, the flux penetrated the film gradually, and formed the critical-state usually found in superconductors with bulk pinning. For  $T < 10$  K, the gradual penetration was interrupted by abrupt invasion of dendritic flux structures. Shown in Fig. 1 is a series of MO images visualizing the distribution of the perpendicular field  $B$  for  $T = 9.6$  K. At fields below 14.5 mT, a gradual flux penetration from the edges took place. The distribution is then similar to the conventional critical-state picture in a perpendicular geometry:<sup>15</sup> the flux concentrates at the edges, seen as a bright contour around the sample, and partly penetrates inwards. The central part and the regions near the corners remain flux-free and appear black on the image. The observed roughness of the flux front is often found in MO studies of superconductors and indicate

the presence of small defects that lead to the fan-like flux patterns. At 15 mT a big dendritic flux structure abruptly invaded the film (middle panel). The properties of such flux dendrites are described in detail in the previous studies.<sup>6,7,9</sup> Here we emphasize that the exact pattern of the dendrite is not reproducible, and thus not related to defects. During the subsequent field increase, the dendritic structure remains seemingly intact, while the flux front continues advancement, like a moving sand dune, and by  $B_a = 36$  mT, it covers the dendrite almost completely, see Fig. 1(bottom).

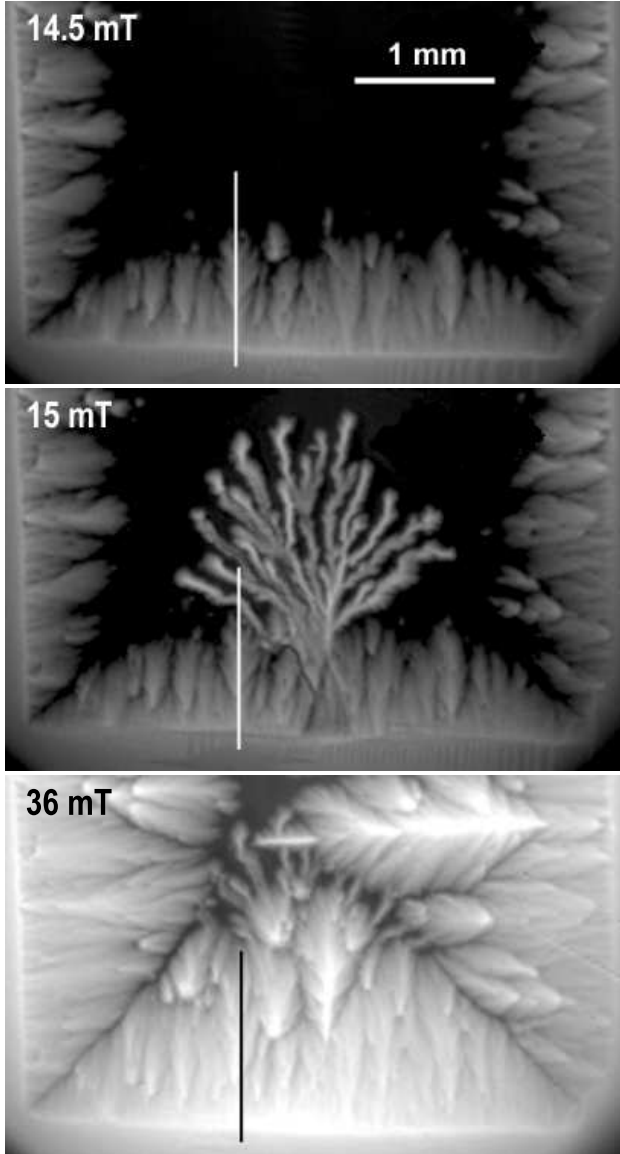


FIG. 1. Magneto-optical images of flux distributions in a  $\text{MgB}_2$  film for increasing applied field (only the lower half of the film is seen). A dendritic structure appeared abruptly at  $B_a \approx 15$  mT.

The evolution of the flux density profiles across the film

during field increase is shown in Fig. 2. The profiles are calculated directly from the MO images along the line indicated in Fig. 1, which is perpendicular to both the film edge and two branches of the dendrite tree. The slope of the profiles is thus everywhere representing the actual  $|\nabla B|$ . The shown profiles cover all the stages of flux penetration: the gradual advancement of flux front into the virgin film (7 and 14.5 mT), the formation of a dendrite (15 mT), and the later gradual penetration covering the dendrite. One can immediately see that for the dendritic branches the profile has an anomalously steep slope. It is therefore tempting to conclude that this corresponds to an anomalously high critical current density. However, an enhanced current density flowing around the branches is bewildering. High as it may be *during* the dendrite formation, the current density should relax fast, and not exceed  $j_c$  flowing in the area of regular flux penetration. In fact, one would expect that the heating accompanying the avalanche reduces the current density.

Even more surprising is the observed evolution of the flux density around a dendrite branch as the flux front is approaching and runs it over, see Fig. 3(top). From the Figure we again notice the anomalously steep slope of the profile across the branch (20 mT curve) compared to the slope after the branch has been wiped out (33 and 39 mT curves). In addition, one finds that the new flux coming to the region from the edge does not simply add up to the existing  $B$  distribution. Instead, it first destroys the existing sharp peak of  $B(x)$ , so that  $B$  is temporarily *decreasing* in the vicinity of the branch core. These two observations are in a strong contrast to the behavior expected in the usual Bean model, see Fig. 3(bottom), where the slopes of  $B(x)$  are fixed, like in a sandpile.

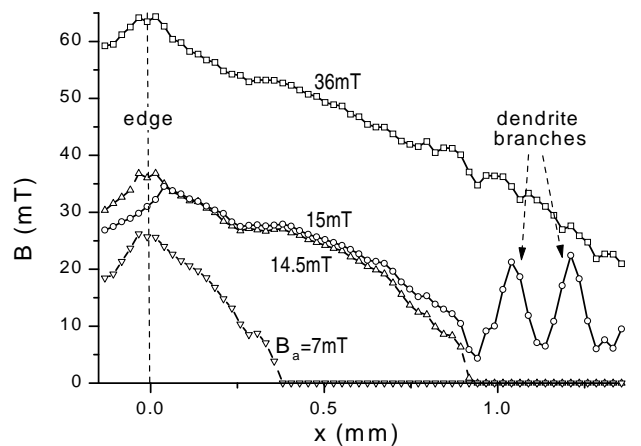


FIG. 2. Profiles of flux density for increasing applied field obtained from MO images along the line shown in Fig. 1. The profile slope across the dendrite branches is much larger than that in other regions and, also larger than in the same region for  $B_a = 36$  mT.

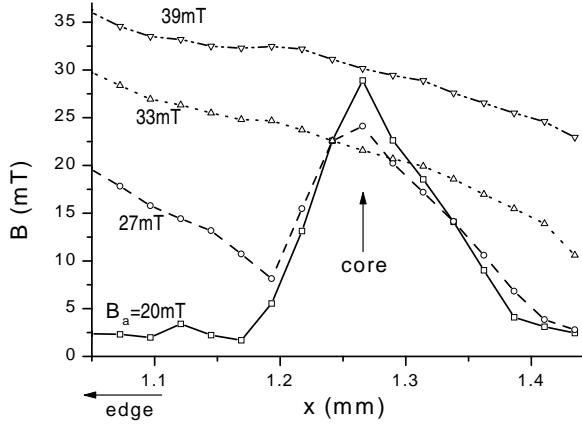


FIG. 3. Top: Profiles of flux density across a dendritic branch for increasing applied field  $B_a$ , where  $x$  is the distance from the film edge. The approaching flux front destroys the critical state around the branch leading to temporal decrease of local flux density in the peak region. Bottom: Behavior expected for a sandpile or the Bean model in parallel geometry, which contrasts the experimental results.

### III. SIMULATIONS

To seek an explanation for the surprising observations we take into account the fact that our sample is a thin film. In such a perpendicular geometry the relation between  $B$  and  $j$  is non-local, and this might be responsible for the experimental behavior shown in Fig. 3. We address the problem by calculating the evolution of  $B$  and  $j$  distributions for the case of flux front approaching a dendritic branch, using flux creep simulations. Focus is set on the flux profile development after the dendrite is formed, while the dendritic branch itself is introduced “by hand” at certain applied field.

Consider a thin film strip with width  $2w$  along the  $x$ -axis, and thickness  $d$  along the  $z$ -axis. We assume  $d \ll w$  and neglect variation of all quantities throughout the strip thickness. A magnetic field applied perpendicular to the strip will then induce a sheet current  $J = dj$ , and an electric field  $E$  directed along the  $y$ -axis. From the Maxwell equation, one has

$$\partial B / \partial t = -\partial E / \partial x. \quad (1)$$

Superconductors in the flux creep regime are usually described by the current-voltage relation,

$$E(J, B) = v_0 |B| |J/J_c|^n \operatorname{sgn} J, \quad (2)$$

where  $n \gg 1$ , and has the meaning of a vortex depinning activation energy divided by  $kT$ ,<sup>17</sup> and  $v_0$  is the vortex velocity at  $J = J_c$ . Finally, the nonlocal relation linking the current and flux density distributions in the strip reads<sup>18</sup>

$$\mu_0 J(x) = \frac{2}{\pi} \int_0^{2w} \frac{B(x') - B_a}{x - x'} \sqrt{\frac{w^2 - (x' - w)^2}{w^2 - (x - w)^2}} dx'. \quad (3)$$

The simulations start with zero initial conditions,  $B(x, 0) = E(x, 0) = J(x, 0) = 0$ , and for  $t > 0$  the applied magnetic field is assumed linearly increasing in time,  $B_a = \dot{B}_a t$ . To provide correspondence with the experiment, the field ramp rate was very slow:  $\dot{B}_a \ll B_c v_0 / w$ , where  $B_c = \mu_0 J_c / \pi$  is a typical values for the flux density. The evolution of flux and current density distributions  $J(x, t)$ ,  $B(x, t)$  is then calculated numerically from Eqs. (1)-(3). At the field  $B_a = B_a^*$  a dendritic branch parallel to the film edge is introduced by setting

$$B(x) = \alpha B_a^*, \quad x_0 \leq x \leq x_0 + \Delta, \quad (4)$$

where  $x_0$  and  $\Delta$  give the location and width of the branch. Physically, this is equivalent to having the region  $x_0 \leq x \leq x_0 + \Delta$  instantly heated to the normal state so that it becomes uniformly penetrated by flux with a density proportional to the applied field  $B_a^*$ , where the coefficient  $\alpha$  is determined by the demagnetization factor. The simulations then continue with the same parameters, i.e., we assume that the heated region cools down immediately. To mimic our actual experimental situation, seen in Fig. 2, the following parameter values were chosen:  $x_0/w = 0.5$ , i.e., the dendrite is formed halfway to the film center, at the applied field  $B_a^* = 0.58 B_c$  when the flux front is located at  $\approx 0.75 x_0$ , and to have appropriate height and width of the peak at  $x_0$  we set  $\alpha = 2$  and  $\Delta/w = 0.03$ .

Let us first analyze the distributions for the right half of the strip, where almost no disturbance is created by the dendrite, see Fig. 4. These profiles demonstrate a familiar scenario of flux penetration in the perpendicular geometry: nonlinear  $B(x)$  with a flux front advancing deeper and deeper as  $B_a$  increases, and essentially uniform  $J(x)$  in the flux penetrated area and a considerable current also in the Meissner state central part.<sup>19</sup> Such profiles are often found in MO studies of thin superconductors,<sup>16</sup> and were obtained by flux creep simulations already long ago.<sup>20</sup> The profiles are also very close to the Bean-model result for a thin strip,<sup>18,21</sup> which is expected for the large  $n = 25$  used in the present simulations.

Next, we examine the left side of the strip, and how the penetration there is perturbed after the appearance

of the dendrite. The initial rectangular profile, Eq. (4), at  $B_a^*$  relaxes very fast because of the high current density associated with such an artificial  $B(x)$ . After this relaxation one finds a triangular shape of the  $B$  profile across the dendrite – see the thick line in Fig. 4. Note that the left slope of the dendrite is steeper than on the right side, as found also experimentally, see Fig. 3. As the field continues to increase the conventional penetration advances.

It affects drastically the profile around the dendrite. By  $B_a = 0.75B_c$  (dashed line), when the flux front has not yet reached the dendrite, the peak around  $x_0$  is already significantly suppressed. As the field reaches  $0.92B_c$ , any trace of the dendrite has disappeared, and the flux density at  $x_0$  is only half of its original magnitude. Besides, the slope of  $B(x)$  around  $x_0$  became much smaller than for the triangular profile.

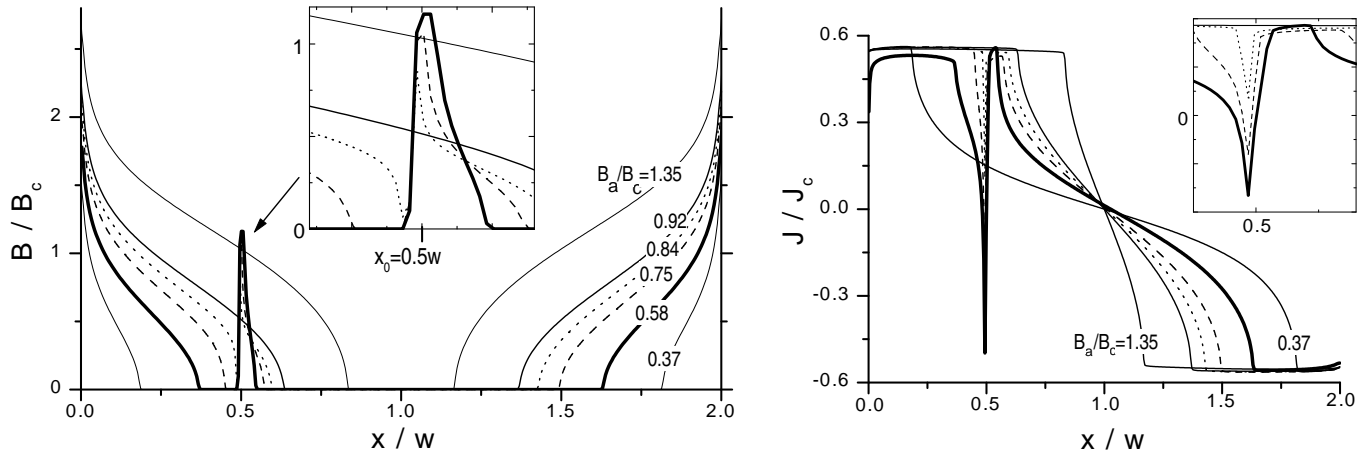


FIG. 4. Flux creep simulations of the evolution of flux and current density in a thin strip under increasing applied field. At the applied field  $B_a^* = 0.58B_c$  a dendritic branch was introduced at  $x_0 = 0.5w$  as described in Eq. (4). The  $B$  profiles are in qualitative agreement with the experimental results shown in Fig. 2 and Fig. 3. The insets show blow-ups of the area near the dendrite.

#### IV. DISCUSSION AND SUMMARY

The present simulations clearly reproduce all main aspects of the experimental behaviour:

- (i) the slope of  $B(x)$  across the dendrite is anomalously steep;
- (ii) the local flux density in the dendrite core temporarily decreases when the flux front approaches;
- (iii) the asymmetry of the triangular profile across the dendrite.

The key to understanding this behaviour lies in the specific  $B - J$  relation for thin strips expressed by Eq. (3). This relation implies an infinite  $\nabla B$  where  $J$  changes abruptly, e.g., near the edge and at the flux front, see Fig. 4. A similar situation is present near the dendrite, where the current changes direction abruptly. Consequently,  $B(x)$  has anomalously high gradient there too, but this is in no way related to having a high local  $j_c$ .

Similarly, the non-locality of Eq. (3) is responsible for smearing out the  $B$  peak at the dendrite. Increasing  $B_a$  induces additional Meissner currents  $J_M$  throughout the whole strip, as schematically illustrated in Fig. 5. As a result, flux motion is activated on the side of the dendrite where the current density was already  $j_c$  (the side most distant from the flux front). The flux motion proceeds in the direction of Lorentz force tending to flatten this side of the peak. Earlier MO experiments have revealed sim-

ilar effects induced by screening currents flowing in the Meissner state region of thin films: unexpected flux dynamics around holes<sup>22</sup> and slits<sup>23</sup> ahead of the advancing flux front.

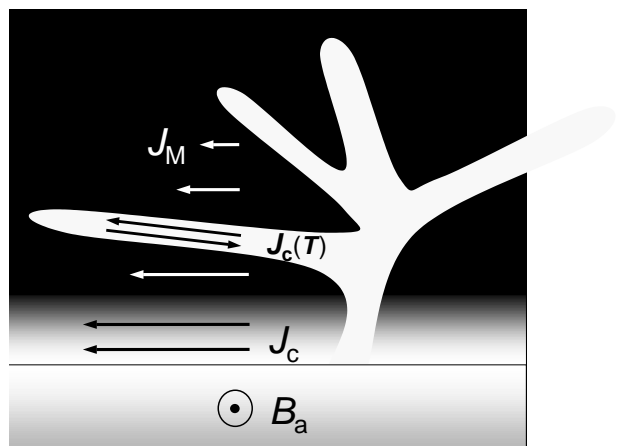


FIG. 5. Schematic of the flux distribution and current flow in a thin film where a flux dendrite is present.

If the critical state around the dendrite were formed at an elevated temperature, the flowing current  $j_c(T)$  would

be correspondingly smaller. As a result, the smearing out of the peak will start at a later stage, i.e., when the flux front is very close to the dendrite. The magnitude of smearing will then also be smaller. In fact, this is what we find by comparing the experiments and simulations. From the Fig. 4 and Fig. 3 we see that the local decrease of  $B$  at the dendrite core is  $\approx 50\%$  in the simulations, but only  $\approx 20\%$  in the experiment. This deviation we believe results from a local heating in the dendrite area during its formation, an effect which was ignored in the simulations.

The work was financially supported by the Norwegian Research Council, NorFa and FUNMAT/UiO.

---

\* Email for correspondence: t.h.johansen@fys.uio.no

- <sup>1</sup> M. R. Wertheimer, J de G. Gilchrist, J. Phys. Chem Solids **28**, 2509 (1967).
- <sup>2</sup> C. A. Duran, P. L. Gammel, R. E. Miller, D. J. Bishop, Phys. Rev. B **52**, 75 (1995).
- <sup>3</sup> V. Vlasko-Vlasov, U. Welp, V. Metlushko, G. W. Crabtree, Physica C **341-348**, 1281 (2000).
- <sup>4</sup> P. Leiderer, J. Boneberg, P. Bruell, V. Bujok, S. Herminghaus, Phys. Rev. Lett. **71**, 2646 (1993).
- <sup>5</sup> U. Bolz, J. Eisenmenger, J. Schiessling, B.-U. Runge, P. Leiderer, Physica B **284-288**, 757 (2000).
- <sup>6</sup> T.H. Johansen, M. Baziljevich, D.V. Shantsev, P.E. Goa, Y.M. Galperin, W.N. Kang, H.J. Kim, E.M. Choi, M.-S. Kim, S.I. Lee, Europhys. Lett. **59**, 599 (2002).
- <sup>7</sup> M. Baziljevich, A.V. Bobyl, D.V. Shantsev, E. Altshuler,

- T.H. Johansen, S.I. Lee, Physica C **369**, 93 (2002).
- <sup>8</sup> A.V. Bobyl, D.V. Shantsev, T.H. Johansen, W.N. Kang, H.J. Kim, E.M. Choi, S.I. Lee, Appl. Phys. Lett. **80**, 4588 (2002).
- <sup>9</sup> F. L. Barkov, D. V. Shantsev, T. H. Johansen, P. E. Goa, W. N. Kang, H. J. Kim, E. M. Choi, S. I. Lee, cond-mat/0205361.
- <sup>10</sup> I. A. Rudnev et al., cond-mat/0211349.
- <sup>11</sup> S. L. Wipf, Cryogenics **31**, 936 (1991).
- <sup>12</sup> R.G. Mints, A.L. Rakhmanov, Rev. Mod. Phys. **53**, 551-592 (1981).
- <sup>13</sup> I. Aranson, A. Gurevich, V. Vinokur, Phys. Rev. Lett. **87**, 067003 (2001).
- <sup>14</sup> W. N. Kang, H. J. Kim, E. M. Choi, C. U. Jung, S. I. Lee, Science **292**, 1521 (2001). 10.1126/science.1060822.
- <sup>15</sup> Ch. Jooss, J. Albrecht, H. Kuhn, S. Leonhardt and H. Kronmüller, Rep. Prog. Phys. **65**, 651 (2002).
- <sup>16</sup> T. H. Johansen, M. Baziljevich, H. Bratsberg, Y. Galperin, P. E. Lindelof, Y. Shen and P. Vase, Phys. Rev. B **54**, 16264 (1996).
- <sup>17</sup> E. H. Brandt, Rep. Prog. Phys. **58**, 1465 (1995).
- <sup>18</sup> E. H. Brandt, and M. Indenbom, Phys. Rev. B **48**, 12893 (1993).
- <sup>19</sup> Note from the  $J(x)$  profiles in Fig. 4 that the apparent critical current density is  $\approx 0.6J_c$ , which is determined by the characteristic electric field  $E = w\dot{B}_a$  and Eq. (2).
- <sup>20</sup> Th. Schuster, H. Kuhn, E. H. Brandt, M. Indenbom, M. R. Koblischka, M. Konczykowski, Phys. Rev. B **50**, 16684 (1994).
- <sup>21</sup> E. Zeldov, J. R. Clem, M. McElfresh, and M. Darwin, Phys. Rev. B **49**, 9802 (1994).
- <sup>22</sup> J. Eisenmenger, P. Leiderer, M. Wallenhorst and H. Dötsch, Phys. Rev. B **64**, 104503 (2001).
- <sup>23</sup> M. Baziljevich, T. H. Johansen, H. Bratsberg, Y. Shen and P. Vase, Appl. Phys. Lett. **69**, 3590 (1996).